

# Effects of Molecular Weight and Arm Number on Properties of Star-Shape Styrene–Butadiene–Styrene Triblock Copolymer

Xiaopeng Xiong,<sup>1</sup> Lina Zhang,<sup>1</sup> Zhaocheng Ma,<sup>1</sup> Yang Li<sup>2</sup>

<sup>1</sup>Department of Chemistry, Wuhan University, Wuhan 430072, China

<sup>2</sup>The Research Institute of SINOPEC Beijing, Yanshan Petrochemical Company Limited, Beijing 102500, China

Received 24 February 2004; accepted 19 July 2004

DOI 10.1002/app.21267

Published online in Wiley InterScience (www.interscience.wiley.com).

**ABSTRACT:** A star-shape styrene–butadiene–styrene triblock copolymer SBS (802) was synthesized and fractionated into four fractions coded as 802-F1 (four arms), 802-F2 (two arms), 802-F3 (one arm), and 802-F4 by repeating fractional precipitation. Their weight-average molecular weight ( $M_w$ ) was measured by size-exclusion chromatography combined with laser light scattering to be  $16.0 \times 10^4$ ,  $8.2 \times 10^4$ ,  $4.3 \times 10^4$ , and  $1.19 \times 10^4$ , respectively. The samples were, respectively, compression-molded and solution-cast to obtain the sheets coded as 802C, 802-F1C, 802-F2C, and 802S, 802-F1S, 802-F2S. The structures and mechanical properties of the sheets were characterized by <sup>1</sup>H-NMR, scanning electron microscope,

wide-angle X-ray diffractometer, tensile testing, and dynamic mechanical thermal analysis. The results indicated that the compression-molded 802-F1C exhibited the higher tensile strength ( $\sigma_b$ , 28.4 MPa) and elongation at break ( $\epsilon_b$ , 1610%), and its optical transmittance is much higher than those of 802C and 802-F2C. This work revealed that the star-shape SBS with four arms could be helpful in the enhancement of the properties as a result of good miscibility of the compression-molded SBS sheets. © 2004 Wiley Periodicals, Inc. *J Appl Polym Sci* 95: 832–840, 2005

**Key words:** star-shape styrene–butadiene–styrene; copolymer; arm number; mechanical properties

## INTRODUCTION

Recently, block copolymers have attracted much attention because of their prospecting application.<sup>1</sup> For example, since Shell Co. synthesized styrene–butadiene–styrene triblock copolymer (SBS) in 1965, it has been broadly utilized in many fields such as thermoplastic elastomers.<sup>2</sup> There are linear and star-shape SBS in the types of block copolymer. Many studies on the linear SBS have been reported, involving the rheology of the concentrated solution,<sup>3</sup> the diffusion motions, and microphase separation in the dilute solution region.<sup>4,5</sup> It is worth noting that the utilization of SBS and its blends greatly depends on their mechanical properties and processing conditions, which are decided by the morphology of microphase-separated structures in SBS copolymer.<sup>6–8</sup> Flosenzier and Torkelson<sup>9</sup> reported the effects of molecular weight and composition on the morphology and mechanical properties of linear SBS/polystyrene/mineral oil blends, indicating that the mechanical properties heavily depend on the

molecular weight of the homopolystyrene. Feng et al.<sup>10–12</sup> studied the miscibility, microstructure, and dynamics of blends containing different molecular weight homopolystyrene and linear SBS or star-shape SBS using dynamic mechanical analysis, <sup>13</sup>C CPDAS NMR, and small-angle X-ray scattering. The results indicated that the miscibility and the mechanical properties of the blends strongly depended on the molecular weight of homopolystyrene or polystyrene block in SBS copolymer. The star-shape copolymers have been extensively studied because of their good properties.<sup>13–16</sup> However, the effects of the molecular weight and arm number of the star-shape SBS on mechanical and optical properties have been scarcely published.

We have accumulated experience in the fractionation and molecular weight characterization of polymers,<sup>17–19</sup> so we are able to investigate the effect of molecular structure on the properties of copolymers. In this work, we attempt to fractionate a star-shape SBS to obtain fractions with different molecular weight and arm number and then prepare their sheets. The effects of molecular weight and arm number on mechanical properties, microstructures, and optical properties were investigated and discussed. This is the first report on the correlation of molecular weight and arm number to physical properties of the star-shape SBS copolymers.

Correspondence to: L Zhang (lnzhang@public.wh.hb.cn).

Contract grant sponsor: Research Institute of Beijing Yanshan Petrochemical Corp.

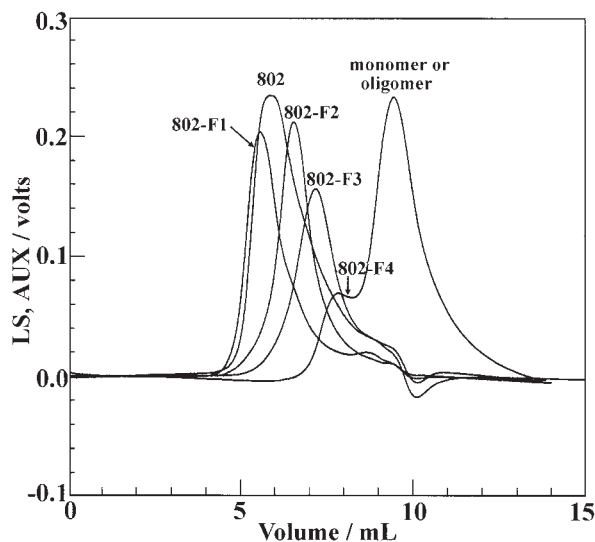


**Figure 1** The SEC chromatograms of the star-shape SBS and its fractions.

## EXPERIMENTAL

### Synthesis of star-shape SBS copolymer

All raw materials used in this work were purified prior to their use. Styrene, butadiene, and *n*-butyllithium were self-made in Yanshan Petrochem. Co. in China. Cyclohexane (from Jinxi Chemical Plant, China) was treated with 5-Å molecular sieves and then deoxygenated.  $\text{SiCl}_4$  was analysis degree and purchased from 57,601 Chemical Plant (Beijing, China).

All polymerization experiments were carried out under a 5-L air-free kettle condition. Based on sequential anionic "living" copolymerization, 40% (w/w) styrene was dissolved in cyclohexane with stirring and then appropriate *n*-butyllithium was added to the solution, resulting in a red color. The homopolymerization of polystyrene was carried out at 50°C for 2 h and then 60% (w/w) butadiene was added to the mixture to obtain poly(S-*b*-B) diblock anions. Finally, the linking agent  $\text{SiCl}_4$  was added to the resulting mixture solution, and the linking reaction was carried out at 50°C for 48 h to

form the star-shape SBS copolymer coded 802. The residual active chains were terminated under a vacuum with ethanol.

### Fractionation

Sample 802 was dissolved in THF at 20°C in a pear flask (0.01 g/mL). Ethanol was gradually added with vigorous agitation at constant temperature until distinct turbidity and then warmed up to 25°C to make it transparent again. The resulting solution was cooled gradually to the original temperature with vigorous agitation and then left overnight to form two phases. The precipitated polymer was separated and then vacuum-dried and coded as the first fraction, 802-F1. Furthermore, more ethanol was added to the remaining solution to obtain the fractions 802-F2 and 802-F3 using the same procedure. The final fraction, 802-F4, was obtained by rotary evaporation of the remaining solution under reduced pressure at 35°C, which was mucus.

### Characterization

Viscosities of the samples were measured at  $25 \pm 0.1^\circ\text{C}$  using an Ubbelohde viscometer, and THF was used as solvent for samples. The kinetic energy correction was always negligible. Huggins and Kraemer plots were used to estimate the intrinsic viscosity ( $[\eta]$ ).

Size exclusion chromatography combined with laser light scattering (SEC-LLS) was carried out on a laser photometer ( $\lambda = 633 \text{ nm}$ ; DAWN DSP, Wyatt Technology Co., Santa Barbara, CA) combined with a P100 pump (Thermo Separation Products, San Jose, CA) equipped with a TSK-gel G4000H6 column ( $7.5 \times 300 \text{ mm}$ ) at 25°C. A spectra system detector (RI-150, TSP) was simultaneously connected. The eluent was THF with a flow rate of 1.0 mL/min. All solutions with a polymer concentration from  $1.0 \times 10^{-3}$  to  $2.0 \times 10^{-3} \text{ g/mL}$  were filtered first with a sand filter, followed by a  $0.45\text{-}\mu\text{m}$  filter (Whatman, England), and then kept in sealed glass bottles before being injected into the SEC column. The refractive index increment ( $dn/dc$ ) of SBS in THF at 25°C

**TABLE I**  
The Composition,  $M_w$ ,  $d$ ,  $[\eta]$ , and Arm Number for 802 and Its Fractions

Sample	PS content (%)	Percentage of fraction (%)	$M_w \times 10^{-4}$	$d$	$[\eta]$ (mL/g)	Arm number <sup>20</sup>
802	40.0	100	15.8	1.33	98.8	Mixture
802-F1	42.0	95.0	16.0	1.23	114.7	4
802-F2	49.3	2.58	8.2	1.35	65.2	2
802-F3	78.4	1.46	4.3	1.29	34.9	1
802-F4	—	0.96	1.19	2.09	—	—

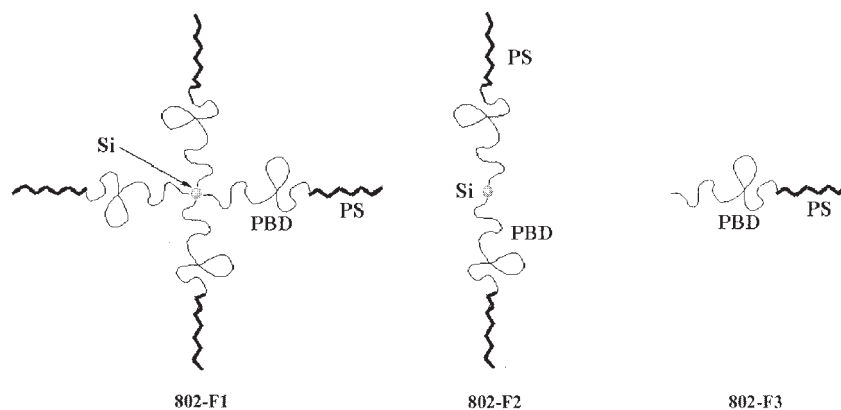


Figure 2 The representation of the molecular structure of 802-F1, 802-F2, and 802-F3.

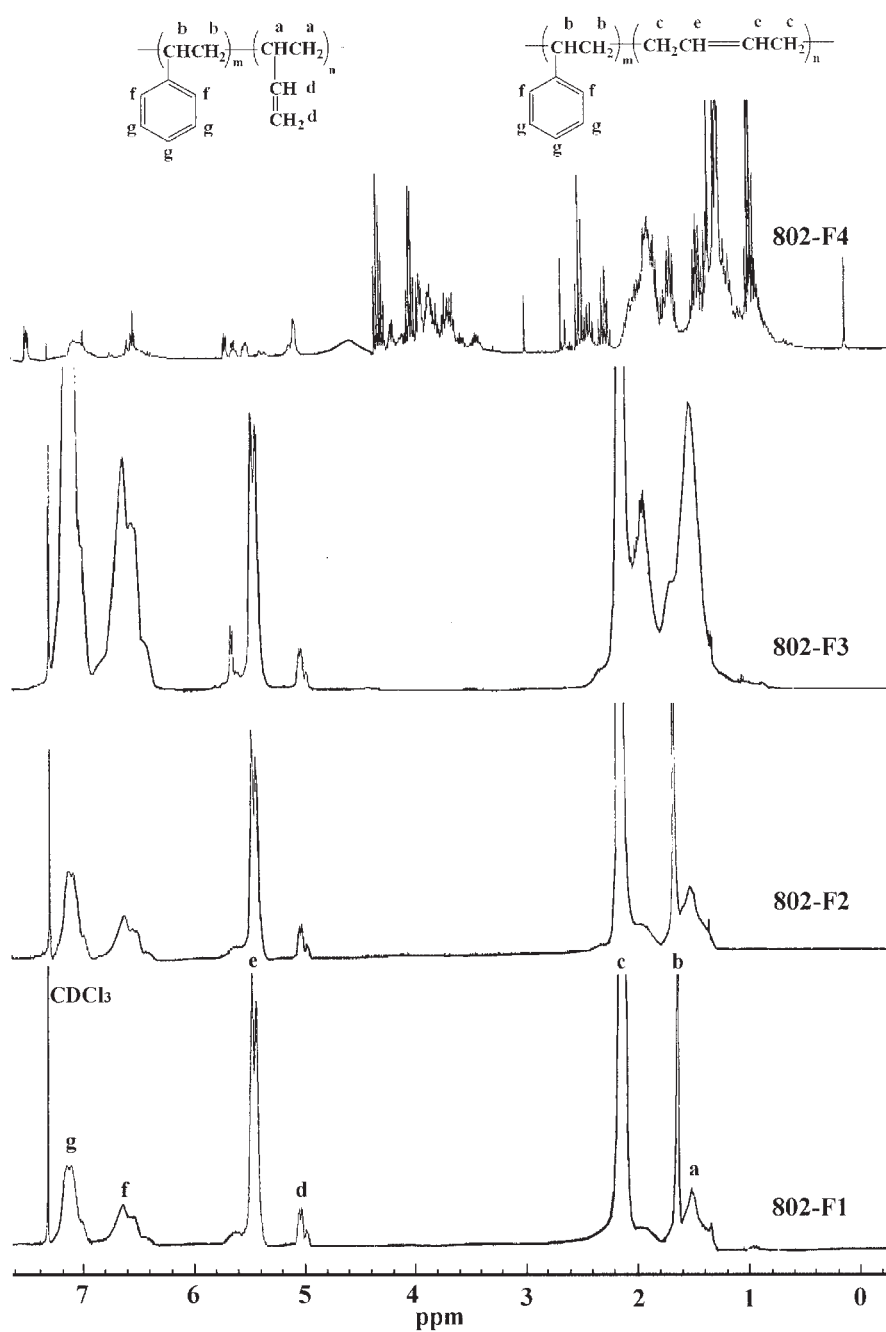
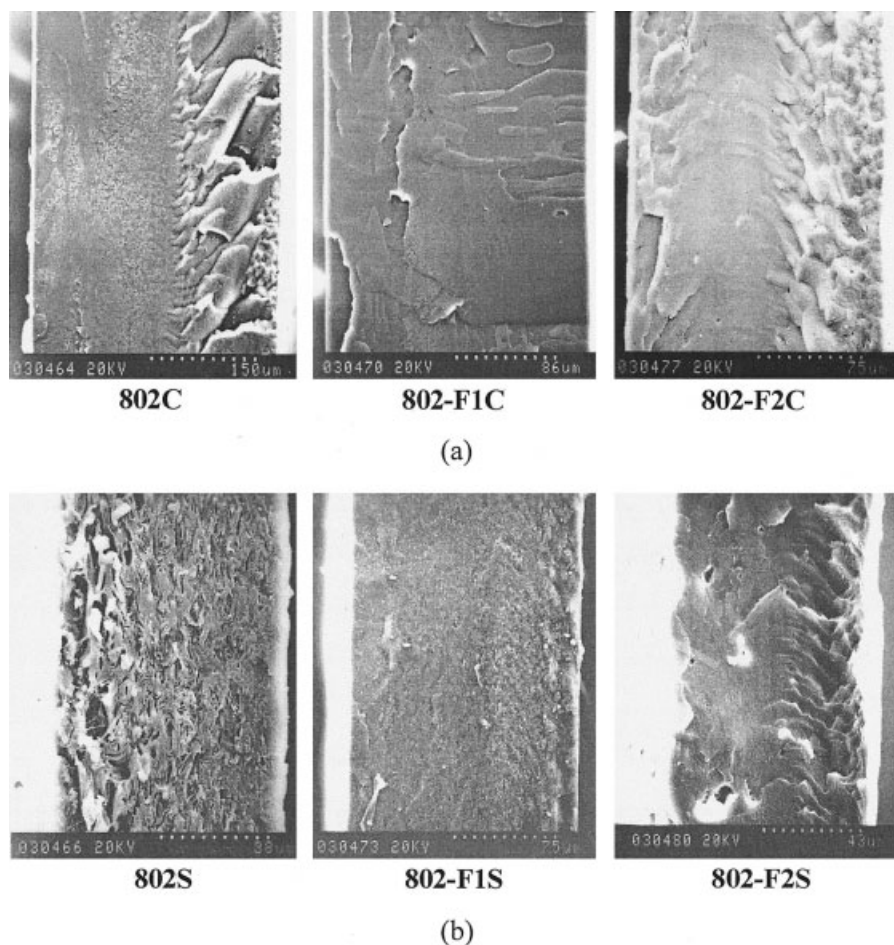


Figure 3 The  $^1\text{H-NMR}$  spectra of the fractions.



**Figure 4** SEM images of the cross section for the compression-molded (a) and cast (b) sheets.

was determined by the optilab refractometer (DAWN DSP, Wyatt Technology Co.) at 633 nm to be 0.145 mL/g. Astra software (Version 4.70.07) was utilized for the data acquisition and analysis.

$^1\text{H-NMR}$  spectra of the fractions were recorded on a Mercury 300 NB NMR spectrometer (Varian Inc.) with  $\text{CDCl}_3$  as the solvent at room temperature. The concentration of the samples was 150 mg/mL.

#### Preparation of sheets

The samples 802, 802-F1, and 802-F2 were cut into small particles with diameter about 0.5 mm and placed in a mold covered with two polished stainless-steel plates. They were molded at  $110^\circ\text{C}$  and 40 MPa for 5 min and then wind-cooled to room temperature for 1 h under constant pressure before removal from the mold to obtain the sheets, coded as 802C, 802-F1C, and 802-F2C, respectively.

To prepare cast sheet, 1 g of 802, 802-F1, and 802-F2 were dissolved in 50 mL THF. The resulting solutions were cast in a petri dish ( $\Phi$  12 cm) at room tempera-

ture and then dried under a vacuum at  $40^\circ\text{C}$  until they maintained a constant weight. The sheets coded as 802S, 802-F1S, and 802-F2S were 0.15 mm in thickness.

#### Measurement of properties

Scanning electron microscopy (SEM) was carried out on a microscope (S-570, Hitachi, Japan). The sheets were frozen in liquid nitrogen and fractured immediately and then vacuum-dried. The fractured surfaces (cross section) of the samples were coated with gold for SEM observation.

Optical transmittances were measured on a UV detector (UV-160, Shimadzu, Japan) with wavelength ranging from 200 to 800 nm. Wide-angle X-ray diffraction (WAXD) patterns of the sheets were recorded on an X-ray diffractometer (XRD-6000, Shimadzu, Japan) with  $\text{Cu K}\alpha$  radiation ( $\lambda = 1.5405 \times 10^{-10}$  m). The samples were examined at  $2\theta$  ranging from  $5^\circ$  to  $40^\circ$  with a scanning rate of  $4^\circ/\text{min}$ .

The tensile testing was performed on a universal tensile tester (CMT6503, Shenzhen Sans Test Machine Co., Ltd., Shenzhen, China) with a strain rate of 100 mm/min at 25°C. The average value of three samples was taken and the experimental error was  $\pm 5\%$  (deviation from the medial value). The sheets were all marked to be 50 mm in length ( $l_0$ ) and then snapped on the universal testing tester previously mentioned with a tensile rate of 100 mm/min. The length ( $l_1$ ) of broken sheets was determined repeatedly after 12-h intervals. The recoverability ( $R_e$ ) of dimension was represented by

$$R_e = (l_0 - \Delta l) / l_1 \times 100\%,$$

where  $\Delta l$  is the length of irrecoverable creep after 12 h and is equal to  $l_1 - l_0$ .

Dynamic mechanical thermal analysis (DMTA) was carried out on a DMTA-V dynamic mechanical analyzer (Rheometric Scientific Co.) at a heating rate of 5°C/min from  $-130$  to  $120^\circ\text{C}$ . The vibration frequency was 10 Hz. The specimens used were about  $15 \times 10 \times 0.15$  mm.

## RESULTS AND DISCUSSION

Figure 1 shows the SEC chromatograms of 802 and its fractions. The fractions contain only one peak except for 802-F4, which exhibits two peaks, corresponding to low-molecular-weight SBS, and components of monomer and oligomers. The molecular weight of 802-F4 was calculated according to the first shoulder peak, and it may be smaller than its true value. The weight percentages of each fraction, the weight-average molecular weight ( $M_w$ ), polydispersity indices ( $d$ ), and  $[\eta]$  for the samples are summarized in Table I. 802-F1, 802-F2, and 802-F3 were composed mainly of four arms, two arms, and one arm, respectively,<sup>20</sup> and their molecular structures are schemed in Figure 2. There is no three-arm SBS fraction detected in the samples. The values of  $M_w$  and  $[\eta]$  are in good agreement with their arm number.

A typical  $^1\text{H-NMR}$  spectrum of styrene-butadiene-styrene triblock copolymer is shown in Figure 3. In the spectrum, two peaks at around  $\delta = 5.0$  (d) and  $5.4$  (e) ppm are assigned to protons of the double bonds of 1,2- and 1,4-butadiene units, and a peak at  $\delta = 1.5$  ppm (a) belongs to the protons of methylene in butadiene units. The peaks at  $\delta$  around  $7.0$  ppm (g and f) are the signals for protons of the phenyl group. The composition of polystyrene (PS) and polybutadiene (PBD) blocks in the copolymer of 802 and the fractions is calculated from the peak intensities (Fig. 2, peaks g, e, and d) and are listed in Table I. It is noted that 802-F1 contains 42.0% PS, which is very close to the composition of 802 (40%, according to the feed composition).

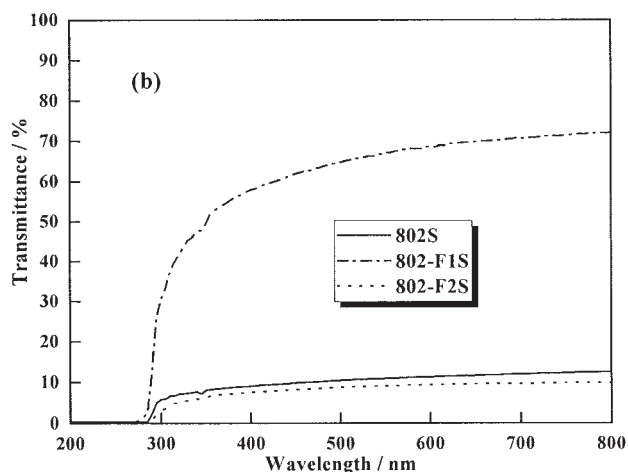
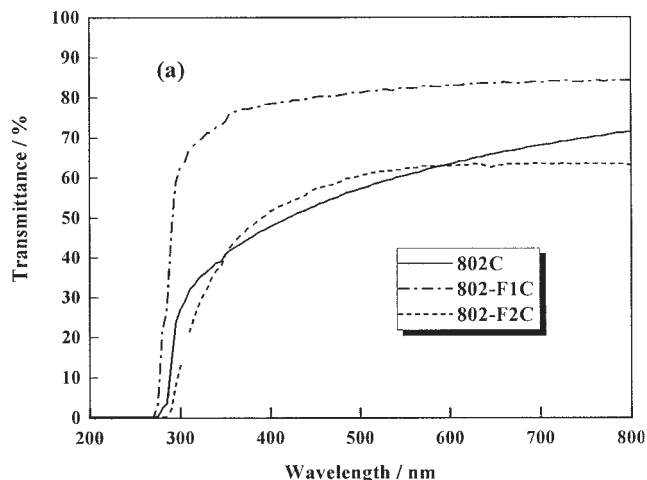


Figure 5 The optical transmittance of the sheets.

The SEM images of the cross section for the sheets are shown in Figure 4. The cross sections of 802-F1C and 802-F1S are smoother than those of 802C, 802S, 802-F2C, and 802-F2S, suggesting that 802-F1C and 802-F1S have better miscibility than the 802 and 802-F2 sheets, which exhibit a phase separation structure. The optical transparencies (Tr) of the compression-molded (a) and cast (b) sheets are shown in Figure 5. The samples exhibit greater than 60% optical transmittance between 400 and 800 nm on the whole. Interestingly, the optical transmittances of 802-F1C and 802-F1S are much higher than those of others, and 802-F1C exhibits the highest light transmittance. The light transmittance measurement is often used as an empirical method for determining the phase separation of materials, which will cause losses in optical transmission because of the quantity of scattered and reflected light at the interface of particles.<sup>17,21–24</sup> The results from SEM and optical transmittance reveal that the miscibil-

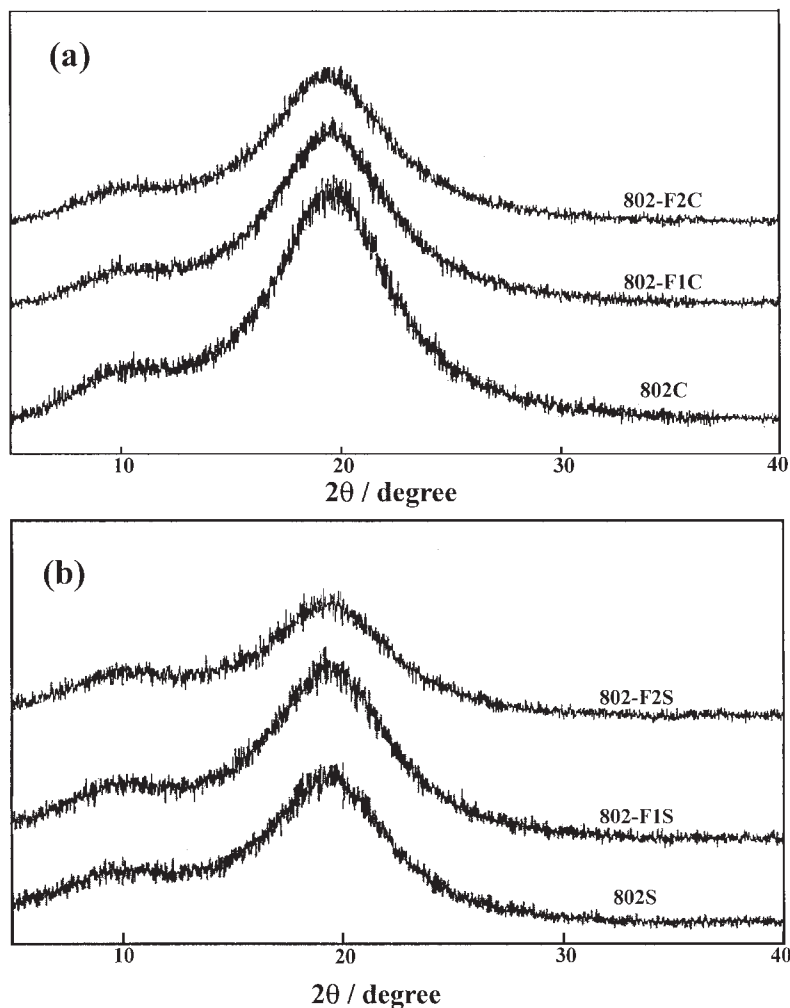


Figure 6 The X-ray diffraction patterns of the compression-molded (a) and cast (b) sheets.

ity of the SBS sheets increases with an increase in arm number. Choi et al.<sup>14</sup> indicated that the phase separation of star-shape poly(ether-ester) block copolymers decreases with an increase of the branching degree. For the compression-molded group, the PS microdomains are destroyed in the molding process, leading to a decrease in phase separation. Figure 6 shows the WAXD patterns of the sheets. No peaks from crystalline diffraction planes were detected, indicating an amorphous structure for all samples. However, the broad peaks suggest some ordered structure, resulting from the microsegregation of phenyl groups in PS.<sup>12,25</sup> The content of the ordered structure (OS) was calculated using the crystallinity calculating method,<sup>25</sup> and the OS values are summarized in Table II. The OS values of the compression-molded sheets are lower than those of the cast sheets because compression molding destroyed the ordered structure. The branching degree of 802-F1 is the highest, so the branching structure hinders the formation of the ordered structure, resulting in the smallest OS values of 802-F1C

and 802-F1S. 802-F2, which is composed of two arms and is a linear polymer, is easier to arrange to form the ordered structures, leading to relatively high OS values. The ordered structure scatters or reflects the light, leading to the decrease of  $T_r$  of 802-F2C and 802-F2S, which is compliant with the optical transparencies results.

Figure 7 shows stress-strain ( $\sigma$ - $\epsilon$ ) curves for the compression-molded (a) and the cast sheets (b). The inset graphs are the megascopic stress-strain curves,

TABLE II  
The Physical Properties of the Sheets

Sample	OS (%)	$\sigma_b$ (MPa)	$\epsilon_b$ (%)	$R_e$ (%)
802C	8.9	10.5	1230	69
802S	17.8	39.8	935	49
802-F1C	12.8	28.4	1610	82
802-F1S	15.3	34.9	1390	68
802-F2C	12.9	8.45	872	58
802-F2S	18.6	9.77	908	43

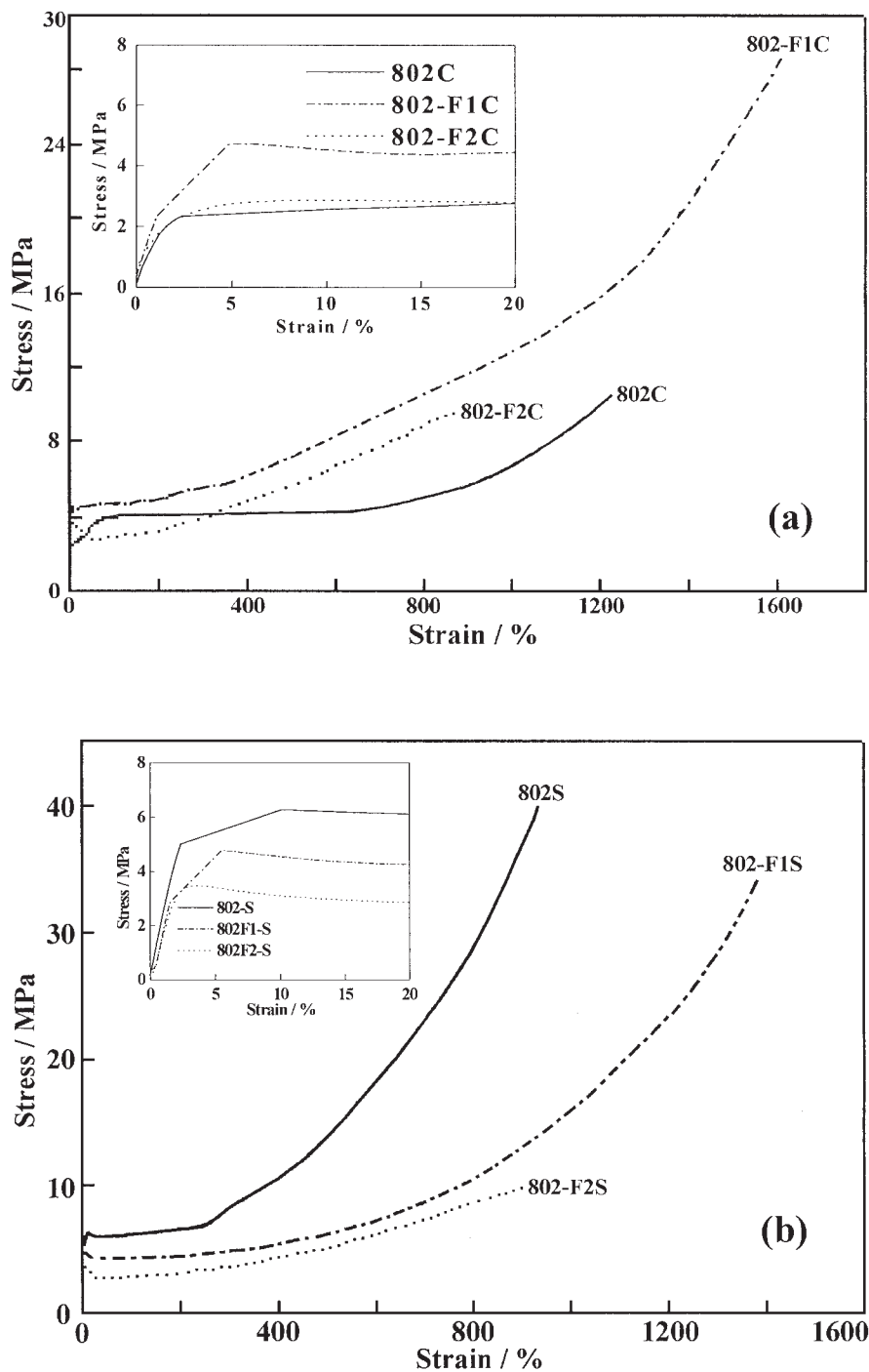


Figure 7 The strain–stress curves of the compression-molded (a) and cast (b) sheets.

and all sheets exhibit the yield points. After a steep increase in stress, an almost constant level is maintained for all samples, and then the stress increases almost linearly with an increase of strain. The abrupt increase of stress is attributed to the deformation of the glassy PS microdomains.<sup>7</sup> This suggests that fracture and segmentation of the glassy PS microdomains take place during the successive strain (400%). However, after completion of the segmentation, the SBS

sheets start to exhibit a typical elastomeric behavior, namely the stress increases with an increase of strain. This is the well-known stain-induced plastic-to-rubber transition.<sup>26</sup> The data of tensile strength ( $\sigma_b$ ), elongation at break ( $\epsilon_b$ ), and  $R_e$  of the sheets are summarized in Table II. Both  $\sigma_b$  and  $\epsilon_b$  for 802-F1C obtained from compression molding are much higher than those of others. Moreover, the four-arm 802-F1C possesses the highest value of  $\epsilon_b$  (1610%). The PS microdomains are

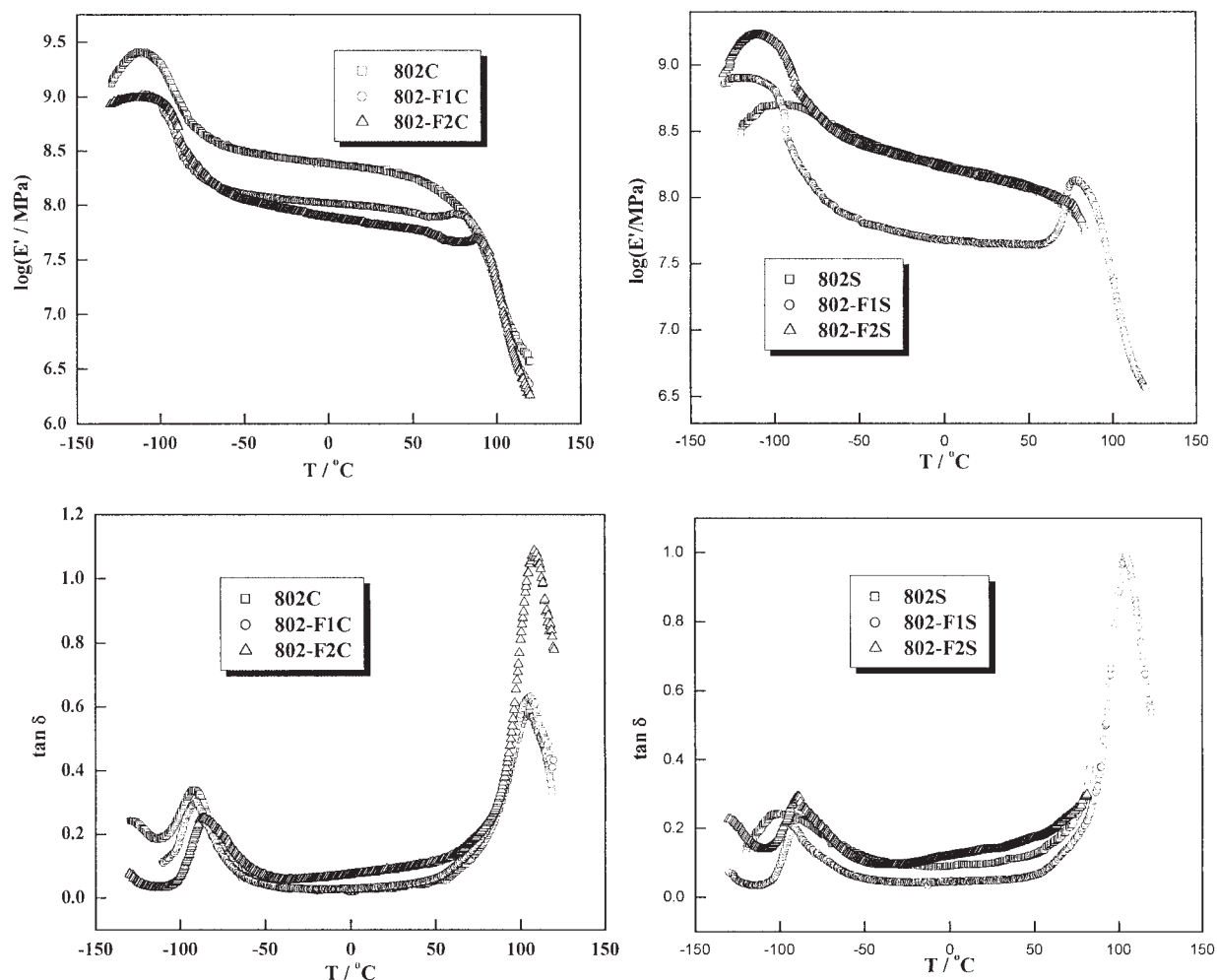


Figure 8 DMTA curves of the sheets.

destroyed when it is melted in the compression-molding processing, and part of them dissolves in the PBD phase to improve the breaking strain. Interestingly, the  $\sigma_b$  of the sheet 802S (39.8 MPa) is the highest. The PS microdomains still exist in the sheet after casting from solution, and the segmented PS microdomains act as physical crosslinks in the rubbery PBD matrix to strengthen the material. Moreover, the PS molecules with low  $M_w$  in SBS could be useful in the formation of physical crosslinks. It is worth stating that the one-arm 802-F3 cannot be prepared to sheet because of low molecular weight. It is obvious that the molecular weight and arm number play an important role in the improvement of the mechanical properties of the SBS sheets. The  $R_e$  values summarized in Table II reveal the same variation tendency as that of the mechanical properties for the SBS sheets.

Plots of storage modulus ( $E'$ ) versus temperature ( $T$ ) and mechanical loss factor ( $\tan \delta$ ) versus  $T$  of the sheets are shown in Figure 8. There are two obvious  $T_g$  values at around  $-90$  and  $105^\circ\text{C}$ , which are assigned to the glass transition temperature of the blocks PBD

( $T_{g1}$ ) and PS ( $T_{g2}$ ), respectively.  $T_{g1}$  values of 802-F2S and 802-F2C shift to a higher temperature than that of 802-F1S and 802-F1C; namely the thermal stability enhances. This can be explained by the fact that the more ordered structures and relatively high content of PS result in the enhancement of  $T_{g1}$  and  $T_{g2}$  for 802-F2S and 802-F2C because of the hindered motions of the PBD and PS chains.<sup>21</sup>  $T_{g2}$  for 802S and 802-F2S cannot be determined, because the samples were melted at higher temperature. This suggests that the 802 sheets prepared by compression molding possess higher thermostability than those prepared by casting.

## CONCLUSION

A star-shape SBS (802) was synthesized and fractionated into four fractions by repeating fractional precipitation. Their  $M_w$  values measured by SEC-LLS were, respectively,  $16.0$ ,  $8.2$ , and  $4.3 \times 10^4$ , corresponding to the arm number such as four, two, and one. The sheet that was compression-molded from the four-arm 802-F1 possessed the highest tensile strength, elonga-



tion at break, and optical transprence and exhibited good miscibility. The phase separation decreased with an increase in arm number. The results revealed that the molecular weight, arm number, and processing conditions play an important role in the improvement of the physical properties of the SBS sheets. The star-shape SBS with four arms could be useful in the simultaneous enhancement of tensile strength, elongation at break, optical transprence, and miscibility of the materials.

## References

1. Legge, N. R.; Holden, G.; Schroeder, H. E. *Thermoplastic elastomers: A comprehensive review*; Hanser: New York, 1987.
2. Medalia, A. I. *Rubber Chem Technol* 1986, 59, 432.
3. Enyiegbulam, M. E.; Hourston, D. J. *Polymer* 1982, 23, 1994.
4. Tsunashima, Y.; Hirata, M.; Kawamata, Y. *Macromolecules* 1990, 23, 1089.
5. Tsunashima, Y. *Macromolecules* 1990, 23, 2963.
6. Sakurai, S.; Iwane, K.; Nomura, S. *Macromolecules* 1993, 26, 5479.
7. Sakurai, S.; Aida, S.; Nomura, S. *Polymer* 2071 1999, 40.
8. Sarkar, M. D.; De, P. P.; Bhowmick, A. K. *Polymer* 1999, 40, 1201.
9. Flosenzier, L. S.; Torkelson, J. M. *Macromolecules* 1992, 25, 735.
10. Feng, H.; Feng, Z.; Yuan, H.; Shen, L. *Macromolecules* 1994, 27, 7830.
11. Feng, H.; Feng, Z.; Shen, L. *Macromolecules* 1994, 27, 7835.
12. Feng, H.; Feng, Z.; Shen, L. *Macromolecules* 1994, 27, 7840.
13. Frater, D. J.; Mays, J. W.; Jackson, C. J.; *Polym Sci B Polym Phys* 1997, 35, 141.
14. Choi, Y. K.; Bae, Y. H.; Kim, S. W. *Macromolecules* 1998, 31, 8766.
15. Tsitsilianis, C.; Voulgaris, D. *Polymer* 2000, 41, 1607.
16. Se, K.; Sakakibara, T.; Ogawa, E. *Polymer* 2002, 43, 5447.
17. Gao, S.; Zhang, L. *Macromolecules* 2001, 34, 2202.
18. Xu, X.; Zhang, L. *Biopolymers* 2002, 65, 387.
19. Zhang, M.; Zhang, L. *Biopolymers* 2001, 59, 457.
20. Zhang, L.; Ma, Z.; Xiong, X.; Ma R.; Li Y. *J Appl Polym Sci*, in press.
21. Krause S. J. *Macromol Sci Rev Macromol Chem* 1972, 7, 251.
22. Weaver, K.; Stoffer, J. O.; Day, D. E. *Polym Compos* 1995, 16, 161.
23. Choudhary, V.; Gupta R. *J Appl Polym Sci* 1993, 50, 1075.
24. Yang, J.; Winnik, M.; Ylitalo, D.; Devoe, R. J. *Macromolecules* 1996, 29, 7047.
25. Feng, H.; Feng, Z.; Yuan, H.; Shen, L. *Macromolecules* 1992, 25, 5891.
26. Kawai, H.; Hashimoto, T. *Contemporary topics in polymer science*; Plenum Press: New York, 1979; p. 245.